

Supplementary information to

Thermal surface chemistry of precursors relevant to focused electron beam induced deposition of iron

[Lars Barnewitz](#),¹ [Hannah Boeckers](#),¹ [Atul Chaudhary](#),² [Lisa McElwee-White](#),² and [Petra Swiderek](#)*¹

Address: ¹Institute for Applied and Physical Chemistry (IAPC), Faculty 2 (Chemistry/Biology), University of Bremen, Leobener Str. 5, 28359 Bremen, Germany, ²Department of Chemistry, University of Florida, Gainesville, Florida 32611, United States

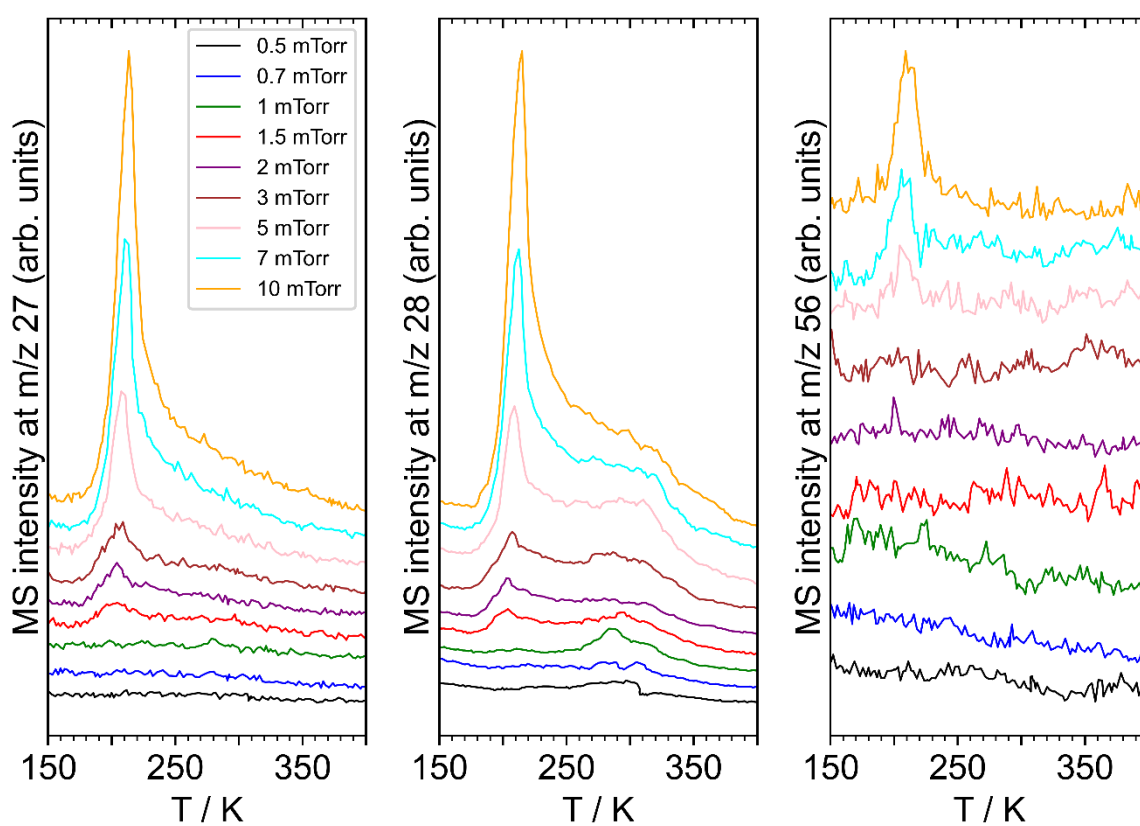


Figure S1. TDS curves obtained for m/z 27 (left), m/z 28 (middle), and m/z 56 (right) after leaking varying amounts of $\text{Fe}(\text{CO})_4\text{A}$ onto the Ta substrate. The gas dose is stated as pressure drop in the gas handling manifold in units of mTorr. Desorption signals near 210 K as indicative of desorption of the intact precursor emerge only above a gas dose of 1 mTorr. This gives evidence that physisorbed multilayers start to form above this gas dose. We note that the MS signal m/z 56 characteristic of Fe^+ is weak and thus rises above the noise level only at higher doses.

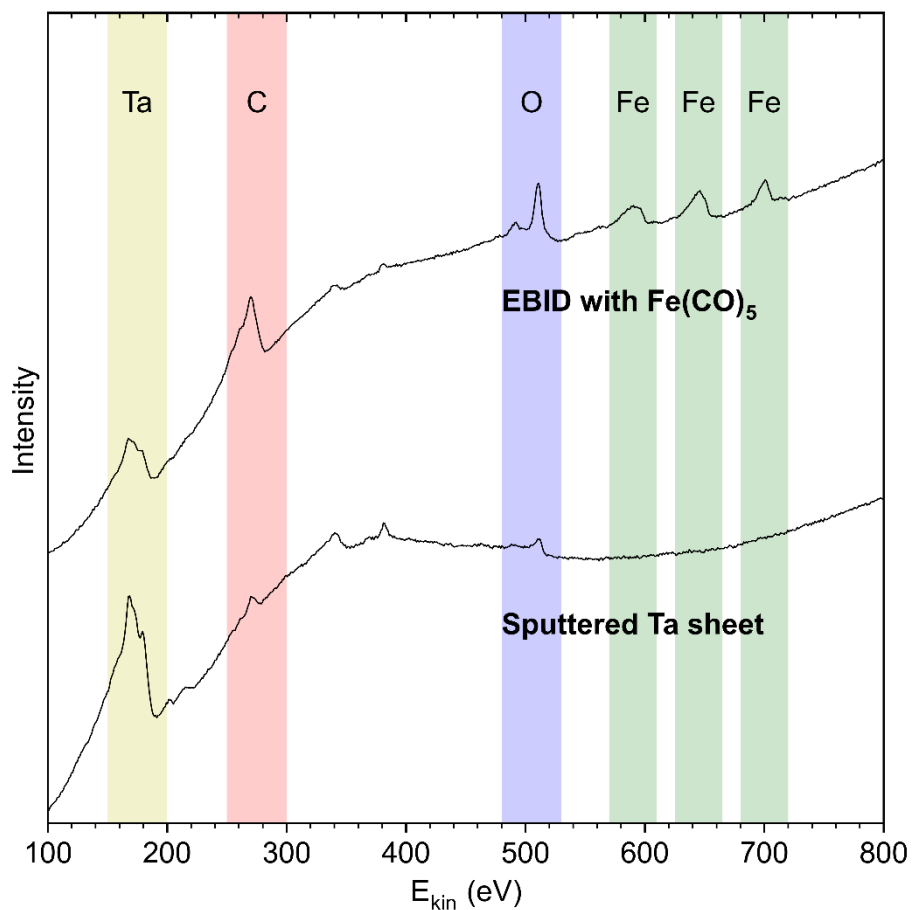


Figure S2. AES recorded with an electron energy of 5 keV on a freshly sputtered Ta substrate (bottom). AES recorded on a deposit produced by dosing $\text{Fe}(\text{CO})_5$ onto the Ta substrate held at room temperature during electron irradiation with an energy of 50 eV while the substrate was held at room temperature (top). The electron dose in the EBID step was $10000 \mu\text{C}/\text{cm}^2$. The amount of $\text{Fe}(\text{CO})_5$ vapor used during the EBID step would have produced a roughly 5 monolayer adsorbate on the substrate if held at 115 K (see Section 2.3 of the main manuscript).

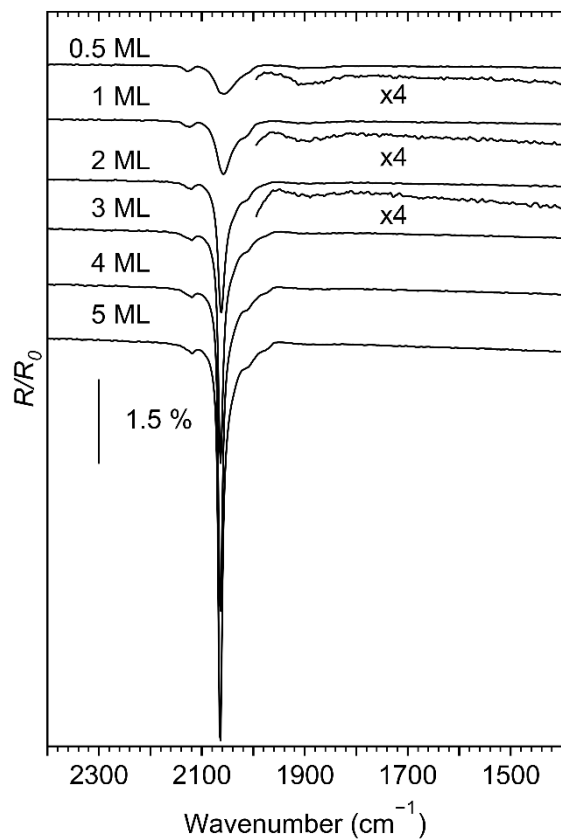


Figure S3. RAIR spectra recorded after repeated dosing of $\text{Fe}(\text{CO})_5$ onto a deposit prepared by EBID from $\text{Fe}(\text{CO})_5$ and held at 115 K. The deposit was prepared as described in Section 3.2 of the main manuscript. n ML denotes the approximate number of $\text{Fe}(\text{CO})_5$ monolayers adsorbed on the deposit after the given sequence of doses. The background for all spectra was recorded prior to precursor dosing.

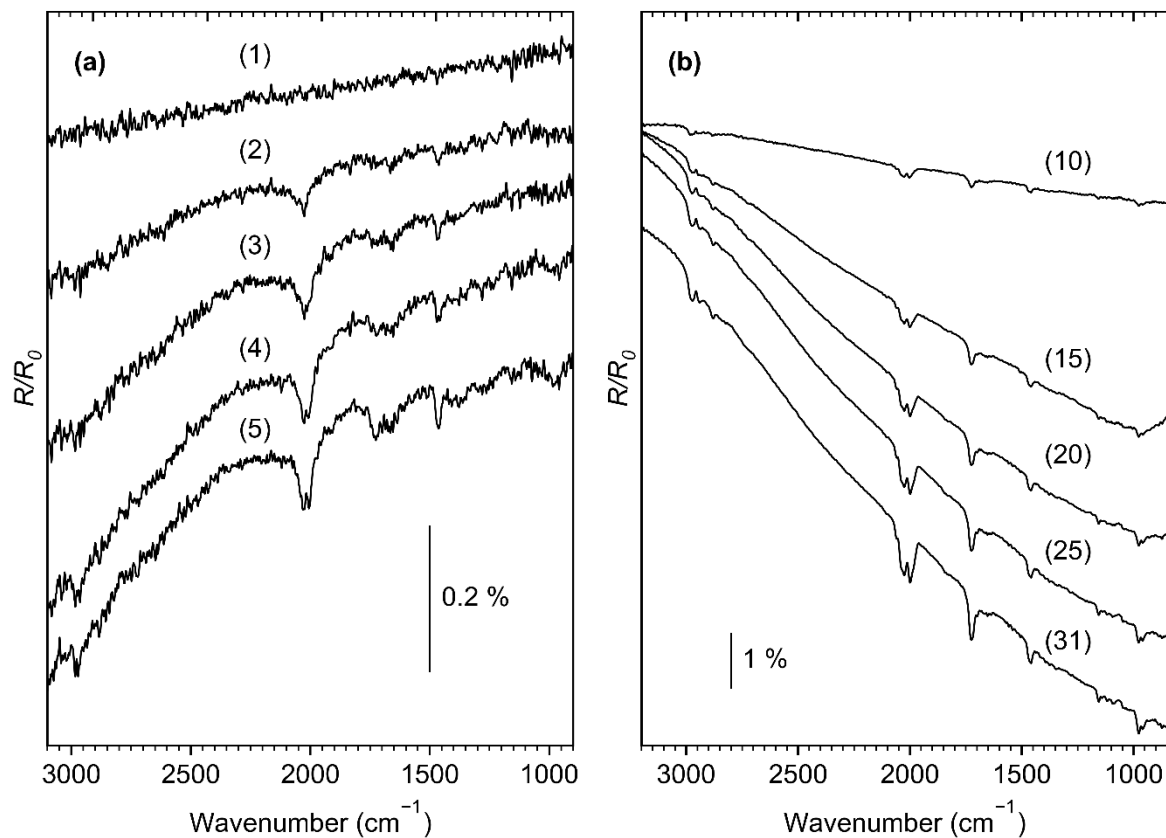


Figure S4. RAIR spectra recorded during continued dosing of $\text{Fe}_2(\text{CO})_9$ onto the freshly sputtered Ta substrate held at 115 K. (a) First five spectra and (b) selected spectra recorded during later stages of dosing. During the dosing process the valves were left open for an extended time period, due to the lower vapour pressure of the compound. RAIR spectra were recorded in approximately 5 min intervals. The values noted next to the spectra denote the time interval during which the spectrum was recorded. The background for all spectra was recorded prior to precursor dosing.

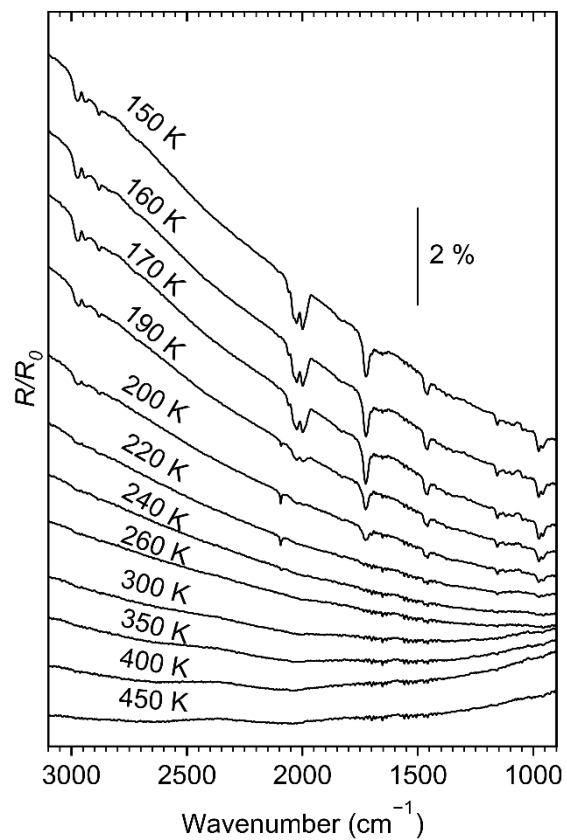


Figure S5. RAIR spectra recorded after annealing of adsorbed Fe₂(CO)₉ to successively higher temperatures. The background was the same as used to record the data of Figure S4.

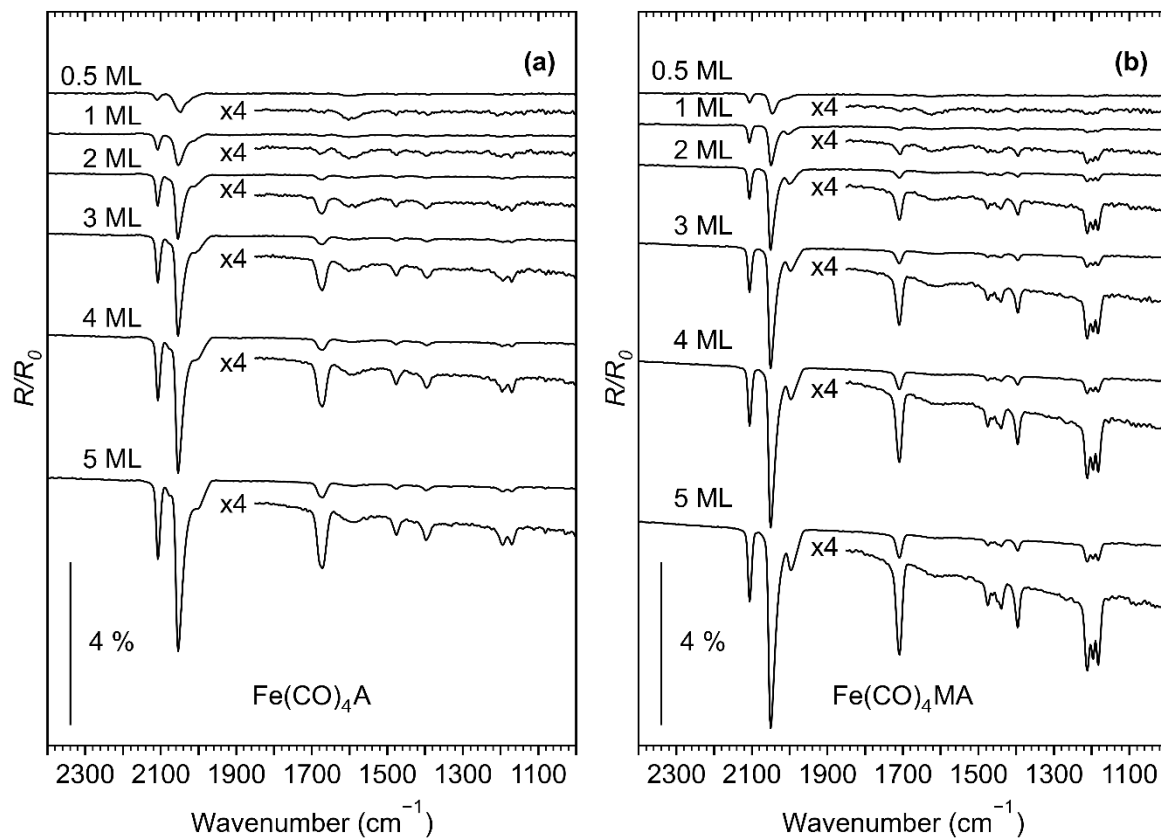


Figure S6. RAIR spectra recorded after repeated dosing of (a) $\text{Fe(CO)}_4\text{A}$ and (b) $\text{Fe(CO)}_4\text{MA}$ onto deposits prepared by EBID from Fe(CO)_5 and held at 115 K. The deposits were prepared as described in Section 3.2. n ML denotes the approximate number of (a) $\text{Fe(CO)}_4\text{A}$ or (b) $\text{Fe(CO)}_4\text{MA}$ monolayers adsorbed on the deposit after the given sequence of doses. The background for all spectra was recorded prior to precursor dosing.

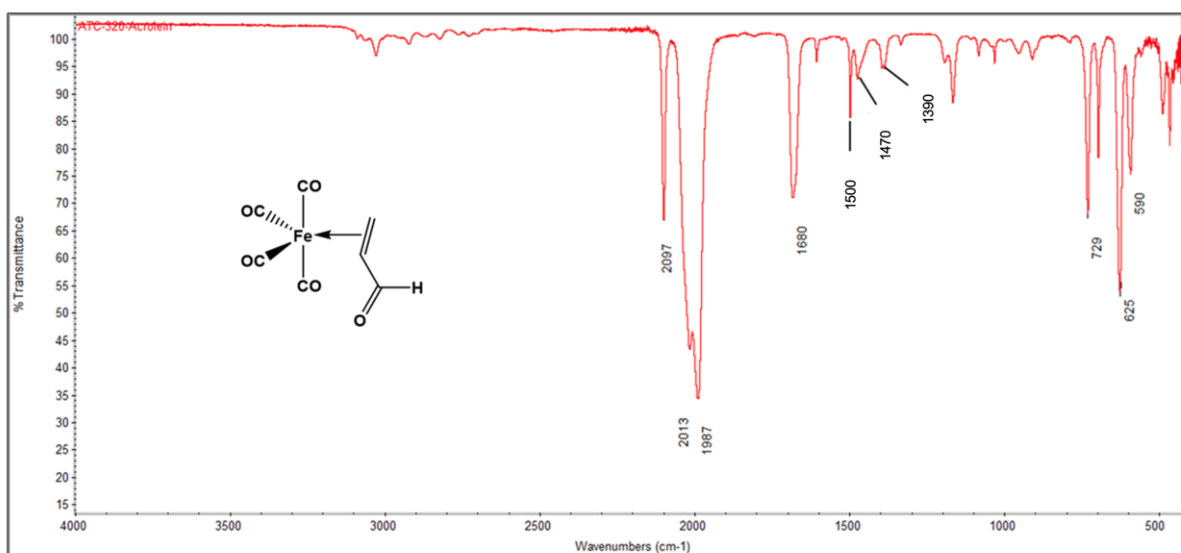


Figure S7. ATR infrared spectrum of Fe(CO)₄A.

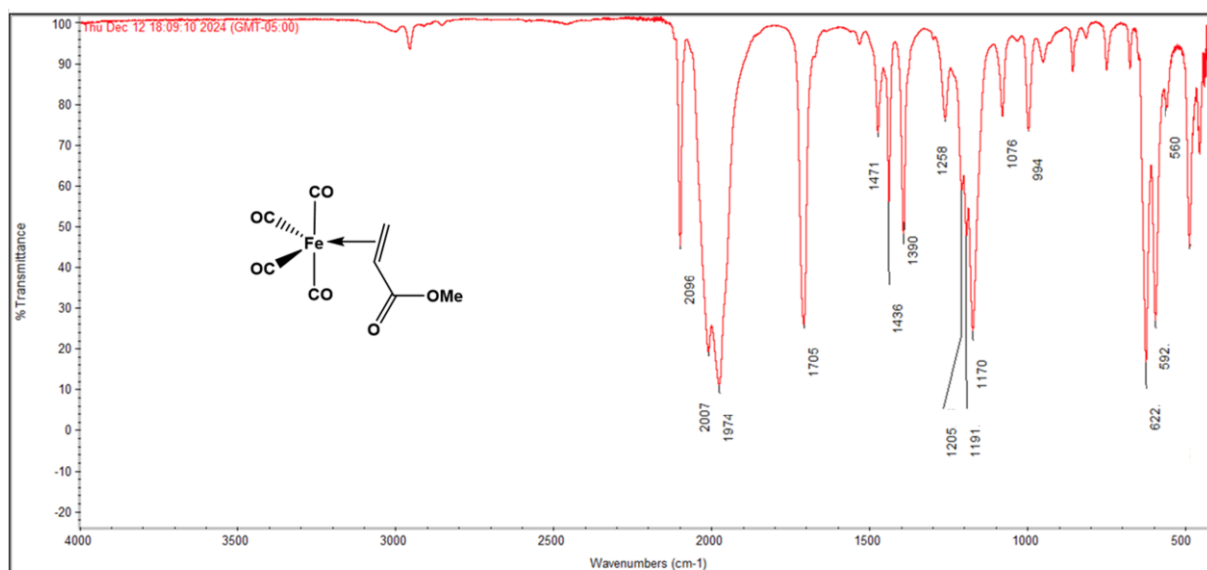


Figure S8. ATR infrared spectrum of Fe(CO)₄MA.

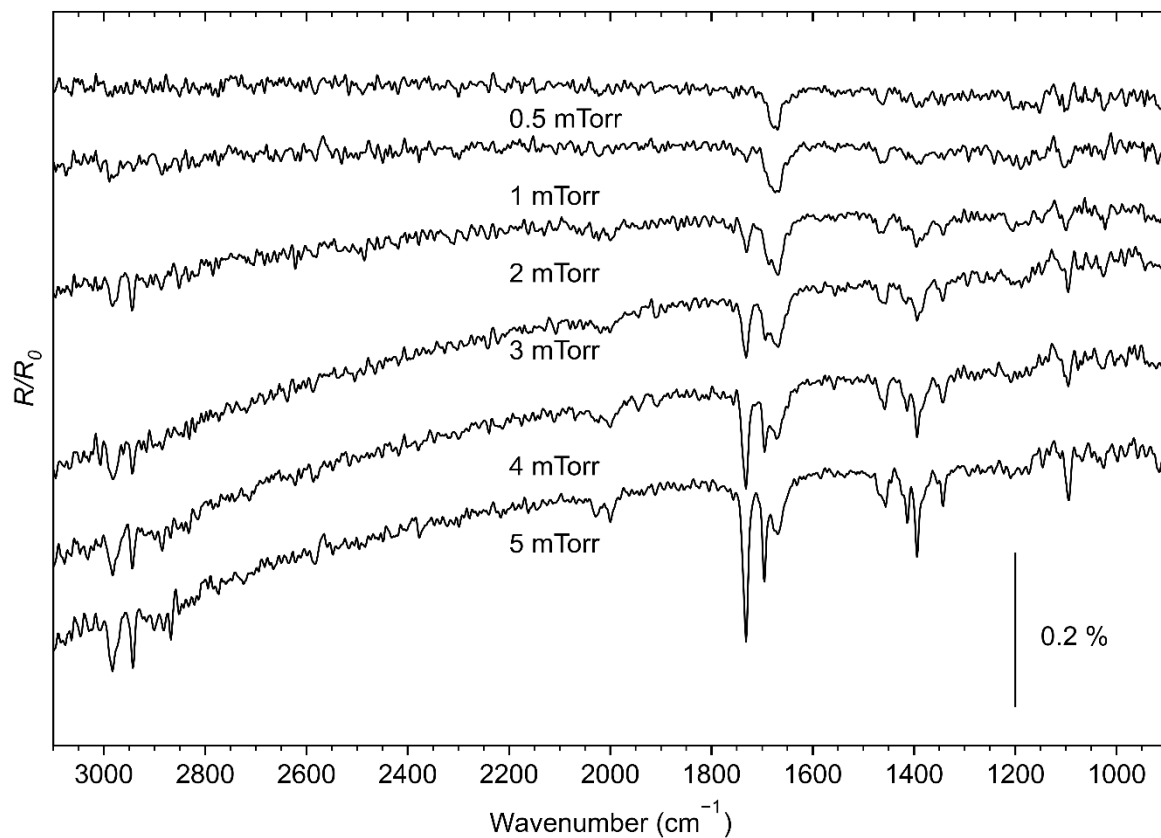


Figure S9. RAIR spectra recorded after repeated dosing of propanal onto a deposit prepared by EBID from $\text{Fe}(\text{CO})_5$ and held at 115 K. The amount of dosed vapour is stated as pressure drop in the gas inlet manifold during leaking the precursors onto the Ta sheet. The appearance of $\nu(\text{C}=\text{O})$ bands at 1695 cm^{-1} and 1730 cm^{-1} at a gas dose of 1 mTorr indicates the onset of multilayer adsorption. The background for all spectra was recorded prior to precursor dosing.

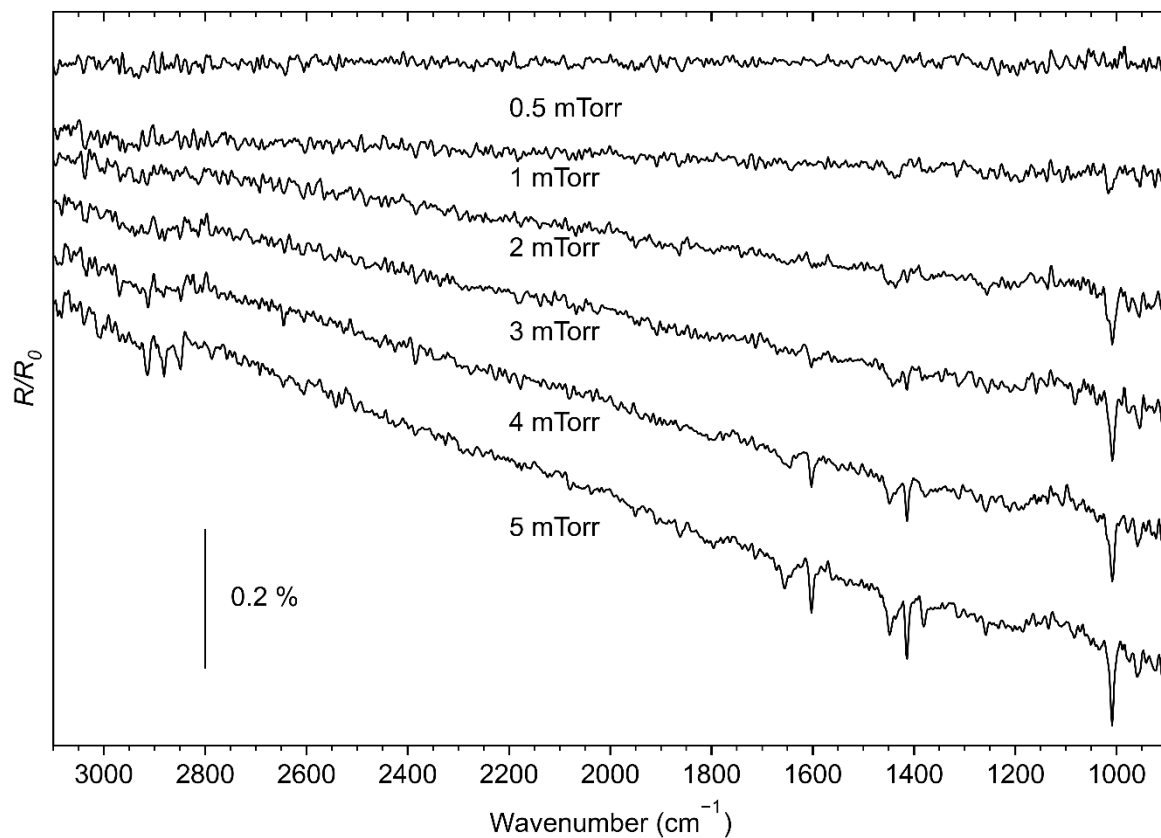


Figure S10. RAIR spectra recorded after repeated dosing of 1,3-pentadiene onto a deposit prepared by EBID from $\text{Fe}(\text{CO})_5$ and held at 115 K. The amount of dosed vapour is stated as pressure drop in the gas inlet manifold during leaking the precursors onto the Ta sheet. From the comparison of the molecular sizes, we tentatively suggest that multilayer adsorption sets in at a similar vapor dose as deduced for propenal in Figure S9. The background for all spectra was recorded prior to precursor dosing.

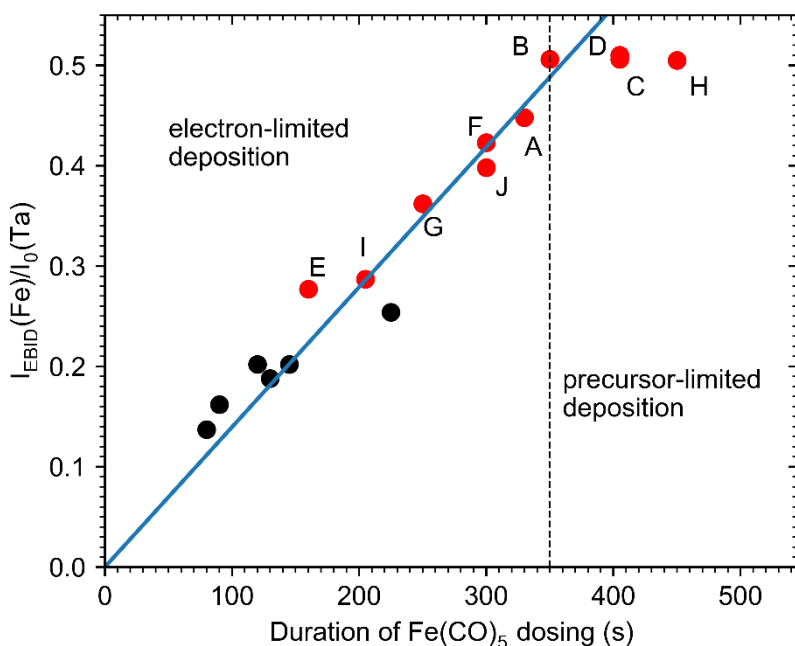


Figure S11. Intensity of the Fe_{LMM} signal after the first EBID step normalized to the intensity of the Ta_{NNN} signal from the freshly sputtered surface prior to EBID as function of the duration of $\text{Fe}(\text{CO})_5$ dosing during the EBID step. Data taken from 16 individual EBID experiments, each performed by dosing of $\text{Fe}(\text{CO})_5$ onto the surface during electron irradiation ($10000 \mu\text{C}/\text{cm}^2$ at 50 eV, lasting for (530 ± 5) s). The total amount of $\text{Fe}(\text{CO})_5$ vapour used in each experiment would have produced a 5 ML adsorbate at 115 K. A-J (red dots) denote the experiments described in Section 3.5.

Table S1. Normalized Fe signal in AES after EBID ($I_{\text{EBID}}(\text{Fe})/I_0(\text{Ta})$) as function of duration of precursor dosing during EBID for 16 individual deposition experiments. $I_0(\text{Ta})$ is the intensity of the Ta_{NNN} signal after sputter-cleaning, $I_{\text{EBID}}(\text{Fe})$ refers to the Fe_{LMM} intensity after the EBID process performed with $\text{Fe}(\text{CO})_5$. A to J refer to the experiments shown in the bar graph of Figure 11 of the main text.

Experiment	$I_{\text{EBID}}(\text{Fe})$	$I_0(\text{Ta})$	Duration of gas dosing [s]	$I_{\text{EBID}}(\text{Fe})/I_0(\text{Ta})$
	12483	61719	145	0.202
	15421	60649	225	0.254
	7868	38993	120	0.202
	6951	36972	130	0.188
D	16307	32255	405	0.506
	6455	39939	90	0.162
	5505	40165	80	0.137
G	13071	36060	250	0.362
H	16964	33611	450	0.505
A	14466	32285	330	0.448
B	15947	31541	350	0.506
E	9379	33917	160	0.277
F	14068	33250	300	0.423
I	9711	33849	205	0.287
J	13679	34411	300	0.398
C	16354	32053	405	0.510